Article

Modeling and Calculation of Improved Centrifuged Reinforced Concrete Columns with Variotropic Structure

Sergey A. Stel'makh [1], Evgenii M. Shcherban' [2], Alexey N. Beskopylny [3,*], Levon R. Mailyan [1], Andrey Veremeenko [4], Aleksandr V. Shilov [5], Oxana Ananova [6], Memduh Karalar [7], Ceyhun Aksoylu [8] and Yasin Onuralp Özkılıç [9,*]

[1] Department of Unique Buildings and Constructions Engineering, Don State Technical University, 344003 Rostov-on-Don, Russia; sergej.stelmax@mail.ru (S.A.S.); lrm@aaanet.ru (L.R.M.)
[2] Department of Engineering Geology, Bases, and Foundations, Don State Technical University, 344003 Rostov-on-Don, Russia; au-geen@mail.ru
[3] Department of Transport Systems, Faculty of Roads and Transport Systems, Don State Technical University, 344003 Rostov-on-Don, Russia
[4] Department of Roads, Faculty of Roads and Transport Systems, Don State Technical University, 344003 Rostov-on-Don, Russia; veremeenko78@mail.ru
[5] Department of Reinforced Concrete Structures, Faculty of Industrial and Civil Engineering, Don State Technical University, 344003 Rostov-on-Don, Russia; avshilov75@mail.ru
[6] Department of Marketing and Engineering Economics, Faculty of Innovative Business and Management, Don State Technical University, 344003 Rostov-on-Don, Russia; o_ananova@mail.ru
[7] Department of Civil Engineering, Faculty of Engineering, Zonguldak Bulent Ecevit University, Zonguldak 67100, Turkey; mkaralar@beun.edu.tr
[8] Department of Civil Engineering, Faculty of Engineering and Natural Sciences, Konya Technical University, Konya 42075, Turkey; caksoylu@ktun.edu.tr
[9] Department of Civil Engineering, Faculty of Engineering, Necmettin Erbakan University, Konya 42000, Turkey
* Correspondence: besk-an@yandex.ru (A.N.B.); yozkilic@erbakan.edu.tr (Y.O.Ö.); Tel.: +7-863-273-8454 (A.N.B.)

Abstract: The use of vibro-centrifugation technology allows the manufacture of variotropic structures that are inhomogeneous in the annular section and have different characteristics along the section thickness. Hardening of the outer layers allows the structure to better resist bending conditions, however, the behavior of the variotropic column under central and eccentric compression remains unexplored. This article considers the problem of compression of hollow columns made of homogeneous concrete that is non-uniform in the annular section (variotropic), and is reinforced with steel reinforcing bars at different values of the load application eccentricity. Variotropic concrete obtained by vibro-centrifugation technology has a stronger outer part and a less durable inner part. The strength of a homogeneous column corresponds to the strength of the middle part of variotropic concrete. The problem was solved numerically in the ANSYS environment for a vertical column rigidly clamped at the bottom edge and loaded with eccentricity at the top edge. Three types of eccentricity are considered; e/r = 0, 0.16 and 0.32 (respectively 0 mm, 0.24 mm and 48 mm). The results of the solution in the form of stress fields, deformations and a pattern of crack development in a spatial setting are obtained. The results showed that for central compression, a homogeneous column has a better bearing capacity of 3.6% than a variotropic one. With the values of eccentricity e/r = 0.16 and 0.32, the variotropic column has a higher bearing capacity (by 5.5% and 6.2%) than the homogeneous one and better resists the development of cracks. The significance of the study lies in the practical application of the proposed approach, developed on a research basis, for non-trivial and complicated operating conditions of columns. This study influences the development of reinforced concrete structures and applies scientific findings to engineering practice.

Keywords: bearing capacity; crack formation; numerical analysis; tubular column; variotropic structure; vibro-centrifugation of concrete

1. Introduction

Modern construction is filled with engineering scientific research in terms of new building structures, solutions and technologies due to the ever-increasing requirements for the safety and functionality of construction projects [1–5]. The decisions made by scientists and engineers can vary. These can be technological solutions that allow the creation of buildings and structures, including increased responsibility, through the introduction of new technologies, expensive equipment and digital computer programs [6–10]. However, an interesting approach involves the search for hidden reserves and unexplored areas in those existing types of structures that are known, but so far have not been taken into account in design, calculation and modeling [11–15]. In this regard, such building structures look promising, which are either known and proposed in regulatory and technical documents, proven and reliable building structures, but with a new approach to them through the use of new materials [16–20]. Or, as the second option, some kind of modernization and improvement of the technology for implementing design solutions is possible, taking into account modern trends in building technologies, structures, calculations and design [21–25]. In works [26–28] the technology of concrete production by the vibro-centrifugation method is proposed. Due to the combined influence of vibration and centrifugal force, an inhomogeneous structure is created, which has increased density and strength at a distance from the axis of symmetry. Such structures are called variotropic and have been studied with various formulations. However, the behavior of variotropic concretes in standard structures, such as columns under central and eccentric compression, is of scientific interest.

Many works are devoted to the study of the behavior of concrete and reinforced concrete columns under axial loading [29–32]. At the same time, numerical simulation methods [33–35], experimental methods [31], and complex methods are widely used to confirm the created models [29,30,36–42]. The material of the columns is also quite diverse in these studies. This can be ordinary reinforced concrete [29,30,32], high-strength concrete [31], high-strength steel-reinforced concrete [30,36], reinforced concrete from steel pipes with concrete filling [33–35,38,40,41], other types of concrete (fiber-reinforced, geopolymer [39], fiberglass [37], and others with various formulation solutions). Differences in existing studies also lie in the size of the columns. The objects of simulation and experimental study were both full-sized [35] and short [36] columns. In addition, mechanical [36] and operational [37] characteristics of columns under the action of axial load were calculated.

In addition to axial loading of concrete and reinforced concrete compressed columns, of great interest to scientists, design engineers and designers is the eccentric application of the compressive load, that is, the presence of the so-called eccentricity of the load application. Here, as well as under axial loading, there is a fairly wide range of studies [32,40,43–57], differing in methods (numerical [46,57], experimental [39,42], complex [25,28,35–37]), material (ordinary and high-strength reinforced concrete [23–26,28], reinforced polymer concrete [50,53], steel fiber-reinforced concrete, carbon fiber-reinforced concrete [51], reinforced concrete from steel pipes filled with concrete [32,40,55–57], and other types of concrete, differing in various formulation solutions, such as the type of binder, filler, additives [49]), the size and shape of the object under study—columns (long [56], short [57], composite [52], square [32,56,57] and round [33,37,41,42]). Of great importance for numerical and experimental studies is also the shape of the section of the column. There are square or round, as well as solid or hollow sections [58–60]. In [61], the influence of the cross-sectional shape and the corner radius on the behavior of prototype columns reinforced with a fiber-reinforced plastic shell during compression was determined. The cross section of the samples changed from square to round as the corner radius increased. It was noted that an increase in the radius of curvature led to a decrease in the stress concentration at the corners of the samples, as a result of which the confining effect of the shell increased and the deformations were more uniform. The highest was the strength of the round section [61]. Particularly interesting for this study are the works devoted to theoretical analysis and numerical modeling of the structural heterogeneity of concrete. In [62], the mechanical properties of multilayer concrete lining for underground structures

with a functional distribution of layers were studied. It has been established that the distribution of stresses in a multilayer concrete lining with a functional arrangement of layers largely depends on the inner radius, thickness and number of layers. The stress concentration decreases with an increase in the number of layers. The ultimate breaking load depended mainly on the concrete strength, Poisson's ratio and the number of layers. Just as in single-layer supports, the destruction of a multilayer support began from its inner face [62]. The authors of [58] studied plane deformations of a hollow multilayer cylinder with a functional distribution of layers. The Airy stress function was used for the study. It was found that in order for the circumferential stress to be uniform across the thickness of the cylinder, the shear modulus must be proportional to the radial co-ordinate. Analytical solutions are presented that can serve as criteria for comparison with approximate solutions obtained numerically [58]. The possibility of optimizing thick-walled viscoelastic hollow polymer cylinders by creating inhomogeneities was considered in [60]. In [63], the possibility of optimizing the parameters of the process for the production of polymer nanofibers by nozzleless centrifugation was studied. The rotation speed of the centrifuge and the parameters of the air flow were varied. During the experiments, the optimal parameters of the rotation speed and air flow, as well as the concentration of the raw solution were determined [63]. In [64], the authors proposed a modified gravitational method for stacking silica particles and ordering the formed colloidal crystals based on centrifugation. The proposed technology made it possible to obtain samples with higher values of reflectivity and structural order than with traditional methods [64].

Combining the topics of concrete heterogeneity and the technology of its production—centrifugation, we will focus on the works [29,65–67]. In [65], the authors studied the effect of a steel shell on the bearing capacity and mechanical characteristics of concrete piles reinforced with a steel pipe. Axial load, surface friction, shaft resistance and head of laboratory-centrifuged pipe-concrete pile samples differed from those for control samples from ordinary reinforced concrete. In particular, the steel shell significantly increased the bearing capacity of the pile shaft, but reduced the strength of the laboratory sample heads, which led to an increase in the overall bearing capacity of the pile, but created potential difficulties for the installation of such piles [65]. The study [66] is devoted to the study of the effect of helical transverse and high-strength longitudinal reinforcement on the physical and mechanical properties of centrifuged reinforced concrete elements of an annular section. Reinforcement parameters and concrete strength varied. It has been established that the flexural and compressive strength in the presence and absence of eccentricity of the application of the load of centrifuged reinforced concrete samples of the annular section to a greater extent depends on the actual strength of the concrete [66]. The study [29] is devoted to an experimental study of the behavior under load during axial compression of centrifuged reinforced concrete columns. The results of the experiments showed that the technology of centrifugation increases the strength of concrete columns by 1.2–2.1 times. The experimental bearing capacity of centrifuged columns was 1.25 times higher than the theoretical value obtained by finite element modeling in the Atena software(Atena V.5.9) package [29]. The compression behavior of hollow sections of centrifugal concrete-filled glass fiber-reinforced polymer (GFRP) pipes was studied experimentally and analytically in [67]. As a result, the influence of the initial eccentricity on the structural characteristics was evaluated. New design equations are recommended for assessing the compressibility of the proposed columns [67].

Thus, the review of the literature revealed a scientific deficit regarding the study of the behavior of compressed reinforced concrete columns that are inhomogeneous in the thickness of the annular section and are subject to off-center loading. The scientific novelty of this study lies in:

- for the first time we have obtained a picture of the stress–strain state of variotropic centrifuged standard reinforced concrete pillars of industrial buildings with the variatropy coefficient taken into account for the first time, that is, the differentiation of concrete properties over the layers of the structure section [68–71];

- assessment of the influence of such variotropy and differentiation of properties on the bearing capacity of such columns, not only in the case of central compression, but especially in the case of eccentricity.
- identifying the relationship between the degree of eccentricity and the efficiency and reliability of such a design;
- comparison of approaches, both normative and the authors', to a general assessment of the bearing capacity of such columns;
- development of a research concept to continue searching for hidden reserves and determine the most effective areas for the work of an unaccounted resource variotropic centrifuged reinforced concrete racks-columns of industrial buildings.

Of course, in order to fully and comprehensively establish the advantage of new types of structures, modern tools should be used. Consequently, the analysis performed shows gaps and insufficient knowledge in the study of the stress–strain state of variotropic columns. Therefore, the purpose of our study is to perform numerical simulation of the operation of promising previously known reinforced concrete structures, namely variotropic centrifuged columns for industrial buildings, as well as to evaluate and identify their hidden resources and reserves. The objectives of our study are to:

(1) perform a number of numerical experiments;
(2) simulate the stress–strain state of variotropic columns under central compression and eccentricity;
(3) identify the features of work depending on a number of different factors affecting this work.

The significance of the study lies in the usefulness of the proposed approach, developed on a research basis, for non-trivial and difficult operating conditions of columns. The influence of the study is felt in the development of previously established postulates of the work of variotropic reinforced concrete structures in compression and in the projection of the obtained scientific results into engineering practice.

2. Materials and Methods

For modeling, a reinforced concrete column was chosen, the diagram of which is shown in Figure 1.

The column is reinforced with eight steel rods with a diameter of 6 mm, evenly distributed around the circumference at the boundary between layers 2 and 3.

The selected column parameters were based on the following aspects: the previous experience of the authors and the prevalence of applied practical applicability of the selected standard sizes, that is, the selected diameter, height and reinforcement scheme of the column are based on popular types of columns from the regulatory framework, and the parameters related to the variability of sections are based on our own research experience.

The heterogeneity (variotropy) of concrete is given by three layers 1, 2 and 3 (Figure 1), which have different mechanical characteristics. The properties of the layers of the variotropic column are chosen in such a way that the inner layer has a lower strength (Table 1). The middle layer has a strength equal to the strength of a homogeneous column, and the outer layer has the highest strength. Such a distribution of strength characteristics is due to the vibro-centrifugation technology and has been experimentally confirmed [26–28].

Modeling was carried out in the ANSYS environment (ANSYS Mechanical 2022 R1). Since the model is symmetric with respect to the *Oxy* plane, only half of it was considered to save computer time. For concrete, 17,280 eight nodal elastoplastic SOLID65 elements were used, for reinforcement—320 beam elastoplastic elements BEAM188 (Figure 1b), which were placed along the lines of the edges of the SOLID65 elements with reference to their nodes. From above, to organize the application of the load, a slab 509 was modeled by elastic elements SHELL43 with a thickness of 100 mm. In total, the model has 18,110 elements and 20,545 nodes. In the process of constructing the mesh of the model, the number of elements was varied over a wide range in order to obtain an acceptable result in a reasonable computation time.
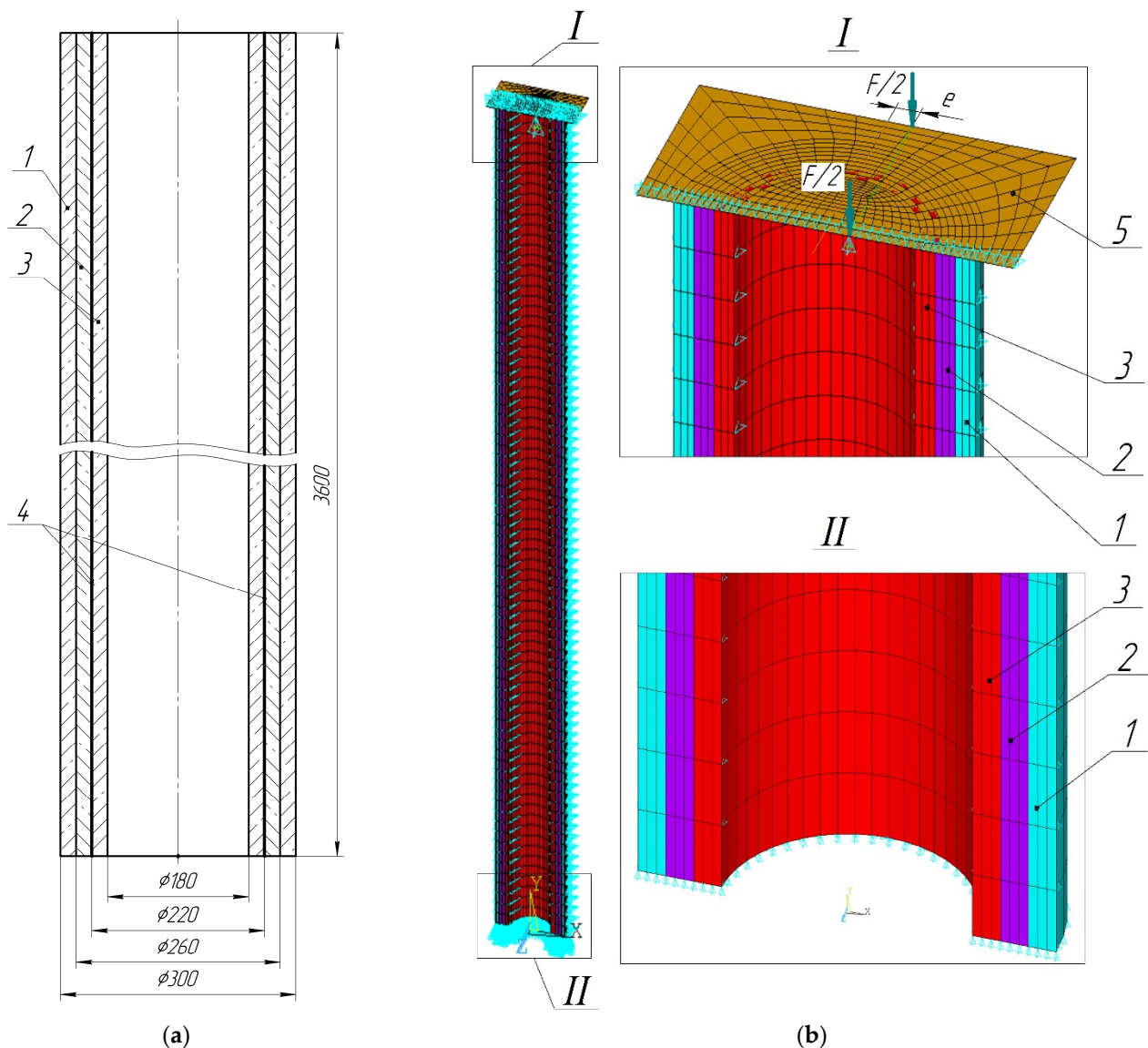
Figure 1. Column scheme (**a**) and FEM model (**b**): 1, 2, 3—concrete layers; 4—reinforcing bars; 5—rigid plate for load transfer with eccentricity. The boundary conditions marked in blue. Other colors correspond to elements with material properties, according to Table 1.

Model boundary conditions:

-   all nodes with coordinate $z = 0$ are fixed along the Oz axis;
-   all nodes with coordinates $y = 0$; $x = 0$ are fixed along the Ox axis;
-   the load is applied by a downward displacement of 2.2 mm to the node with the coordinates $x = e$; $y = l$; $z = 0$ (where e is the load eccentricity; l is the length of the column);
-   nodes with coordinates $x = e$; $y = l$; $z = 0$ and $x = e$; $y = l$; $z = b/2$ are connected in the Oy direction (where b is the top width of the plate).

For analysis, 6 models were built:

-   with homogeneous concrete (homogeneous column) without load eccentricity ($e = 0$);
-   with three-layer concrete (variotropic three-layer column design) without load eccentricity ($e = 0$);
-   with homogeneous concrete (homogeneous column) with load eccentricity ($e = 24$ mm);
-   with three-layer concrete (three-layer column design) with load eccentricity ($e = 24$ mm);
-   with homogeneous concrete (homogeneous column) with load eccentricity ($e = 48$ mm);

- with three-layer concrete (three-layer column design) with load eccentricity (*e* = 48 mm).

Table 1. Mechanical characteristics of model elements.

Number	Title	Characteristics
1	Outer layer	Modulus of elasticity: 4.351×10^{10} Pa Poisson's Ratio: 0.2 Tensile strength: 3.87 MPa Compressive Elasticity: 30 MPa Compressive strength: 38.7 MPa Compressive hardening modulus: 8.610×10^9 Pa
2	Middle layer	Modulus of elasticity: 4.041×10^{10} Pa Poisson's Ratio: 0.2 Tensile strength: 3.32 MPa Compressive Elasticity: 25 MPa Compressive strength: 33.2 MPa Compressive hardening modulus: 6.941×10^9 Pa
3	Inner layer	Modulus of elasticity: 3.721×10^{10} Pa Poisson's Ratio: 0.2 Tensile strength: 2.92 MPa Compressive Elasticity: 20 MPa Compressive strength: 29.2 MPa Compressive hardening modulus: 6.752×10^9 Pa
4	Steel reinforcement	Modulus of elasticity: 2.1×10^{11} Pa Poisson's Ratio: 0.3 Yield strength: 500 MPa Hardening modulus: 870 MPa
5	Plate for eccentrical loading	Modulus of elasticity: 2.0×10^{15} Pa Poisson's Ratio: 0.3.

The elastoplastic properties of concrete and reinforcement were set by a bilinear model with isotropic hardening (Table 1). The properties of the plate (plate) from above are given only by elastic constants.

A non-linear static problem in displacements is considered, while the load was applied to the model from above by displacing the upper nodes of the U_Y model.

The formation and development of cracks in concrete is implemented in accordance with the Willam–Warnke criterion.

$$\frac{F}{f_c} - S \geq 0 \tag{1}$$

where *F* is a function of principal stress state $(\sigma_{xp}, \sigma_{yp}, \sigma_{zp})$; *S* is the fracture surface depending on principal stresses and characteristics of materials; f_c is uniaxial crushing strength, and $(\sigma_{xp}, \sigma_{yp}, \sigma_{zp})$ are principal stresses in principal directions. The presence or absence of a crack is represented according to the Willam–Warnke failure criterion based on the modification of stress–strain relationships by introducing a weakening in the direction normal to the crack face. If a material fails at an integration point under uniaxial, biaxial, or triaxial compression (or tension), it is assumed that the material fails at that point. In SOLID65, crushing is defined as a complete breakdown of the structural integrity of a material. It is assumed that under the conditions when failure occurred, the strength of the material deteriorated to such an extent that the contribution to the stiffness of the element at the considered integration point can be neglected.

3. Results and Discussion

3.1. Numerical Analysis of the Central Compression of the Column (e = 0)

As a result of solving the problem, fields of stresses, displacements, deformations, as well as zones of destruction of concrete were obtained.

Figure 2 shows the dependence of the force acting on the column on the displacement of the upper support. Graphs are presented for the above column options.
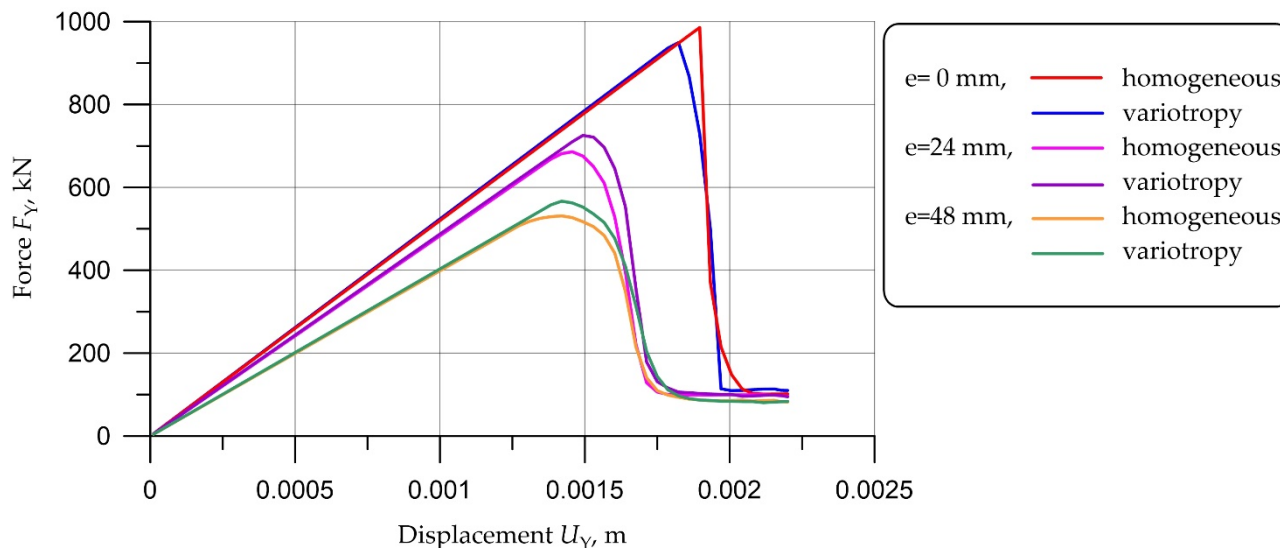

**Figure 2.** Dependences of displacement on force for columns of various designs.

Figure 2 clearly shows several zones of load–displacement dependence. First, the linear dependence $F_Y = f(U_Y)$. Then a non-linear relationship with maximum bearing capacity. At this stage, the destruction of the column begins and a network of cracks appears. In the third zone of supercritical destruction, the bearing capacity of the column drops sharply and the bearing capacity is performed by the reinforcing cage.

The analysis shows (Figure 2) that in the case of central loading, a homogeneous column (red graph) shows greater strength than a three-layer structure column (blue graph), which can be explained by degradation of the remaining sections of the column at the beginning of the destruction of the weakest layer in a three-layer structure.

The variotropic structure has a stronger outer layer, therefore, in the case of an eccentric load application, the situation changes radically, and the best strength results in this case are shown by the variotropic column design (purple and green graphs), which can be explained by the influence of higher strength characteristics in buckling.

Figure 2 clearly shows that in the case of an eccentric load application, the destruction of a homogeneous column begins earlier than a variotropic one. After the start of the destruction of a homogeneous column, the load on it begins to decrease in the process of increasing displacement, in a variotropic column this process begins to occur somewhat later. This load is nothing but a reaction to a force impact. Since the bearing capacity of the column decreases after the beginning of its destruction, the reactive force also decreases, and the deformation continues to grow. This process is also well illustrated by full-scale tests of columns on a press.

The results of solving the problem for a homogeneous concrete structure of a column under central compression (Figure 3a) and a variotropic column (Figure 3b) in the form of equivalent von Mises stress fields show the stress–strain state of the column and the zone of the beginning of destruction (shown in red). It can be seen that the onset of fracture occurs in the upper part of the column, which is due to the influence of the boundary conditions during loading.
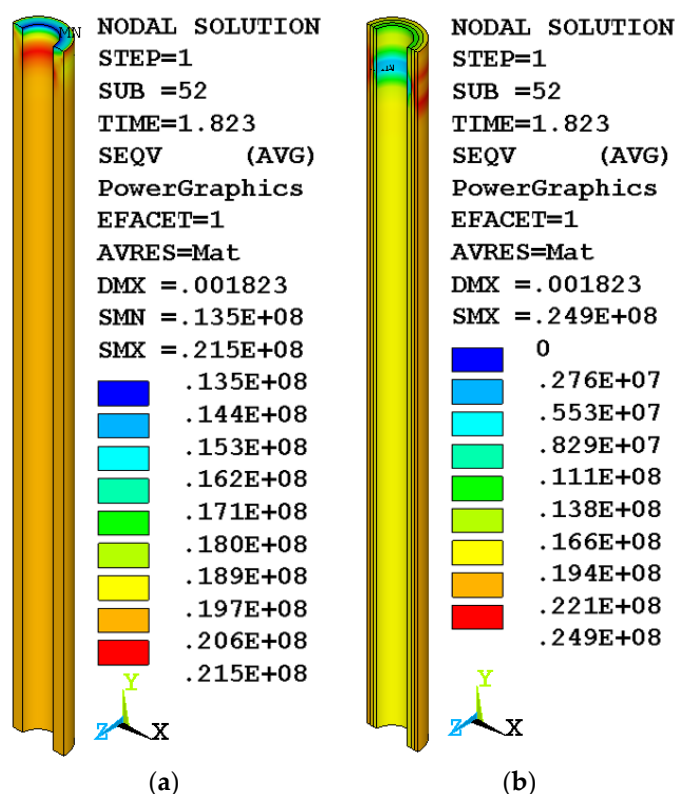
Figure 3. Fields of equivalent stresses in concrete under compression without eccentricity for (**a**) a homogeneous column and (**b**) a variotropic column with a force of 949 N.

Figure 4 shows the formation of cracks in concrete during central compression of a homogeneous column (Figure 4a) and a variotropic column (Figure 4b). It can be seen that in a homogeneous column, cracks are just beginning to appear (Figure 4a), while in a variotropic column, cracks have already developed and the formation of cracks began from the inner surface, that is, the weakest layer. In the case of central compression, cracks are initiated in the inner zones with the lowest compressive strength.

Further loading of the column leads to the beginning of the process of destruction of a homogeneous column and supercritical destruction of the variotropic column (Figure 5a,b respectively). At this stage, the concrete of the variotropic column is practically destroyed, but due to the powerful frame of steel reinforcement, the column still continues to fulfill part of its bearing capacity. It can be seen that a homogeneous column resists external force better, and the crack network (Figure 6a) is less pronounced than for a variotropic column (Figure 6b).

In confirmation of the above, in Figures 5a and 6a it is clearly seen that a homogeneous column under compression by 1.933 mm is in the process of destruction, while the three-layer structure is already almost destroyed (Figures 5b and 6b).

The destruction of a variotropic column begins earlier than a homogeneous one (Figure 3). This can be explained by the fact that when the critical level of stresses in the body of a homogeneous column is reached, the process of its destruction begins with an avalanche-like increase in the loss of the whole (underupted) section. This critical stress background reaches its value immediately over the entire section of the column. In the case of a variotropic column on its inner part, these stresses reach their critical value somewhat earlier than in a homogeneous one (with less displacement, since the strength of the inner layer is less than that of the middle and outer). Consequently, the column begins to collapse precisely here, which leads to a sharp reduction in the area of the remaining surviving section and a faster increase in stresses in it. This is clearly seen in Figures 3 and 5. Moreover, Figure 3 shows the results of loading at step 52, when the intensive process of destruction

of the variotropic column begins (Figure 3b), while in the homogeneous one (Figure 3a), cracks are just beginning to emerge. Cracks are shown in Figure 4a for a homogeneous column and Figure 4b for a variotropic one. Cracks in concrete are marked with red circles.
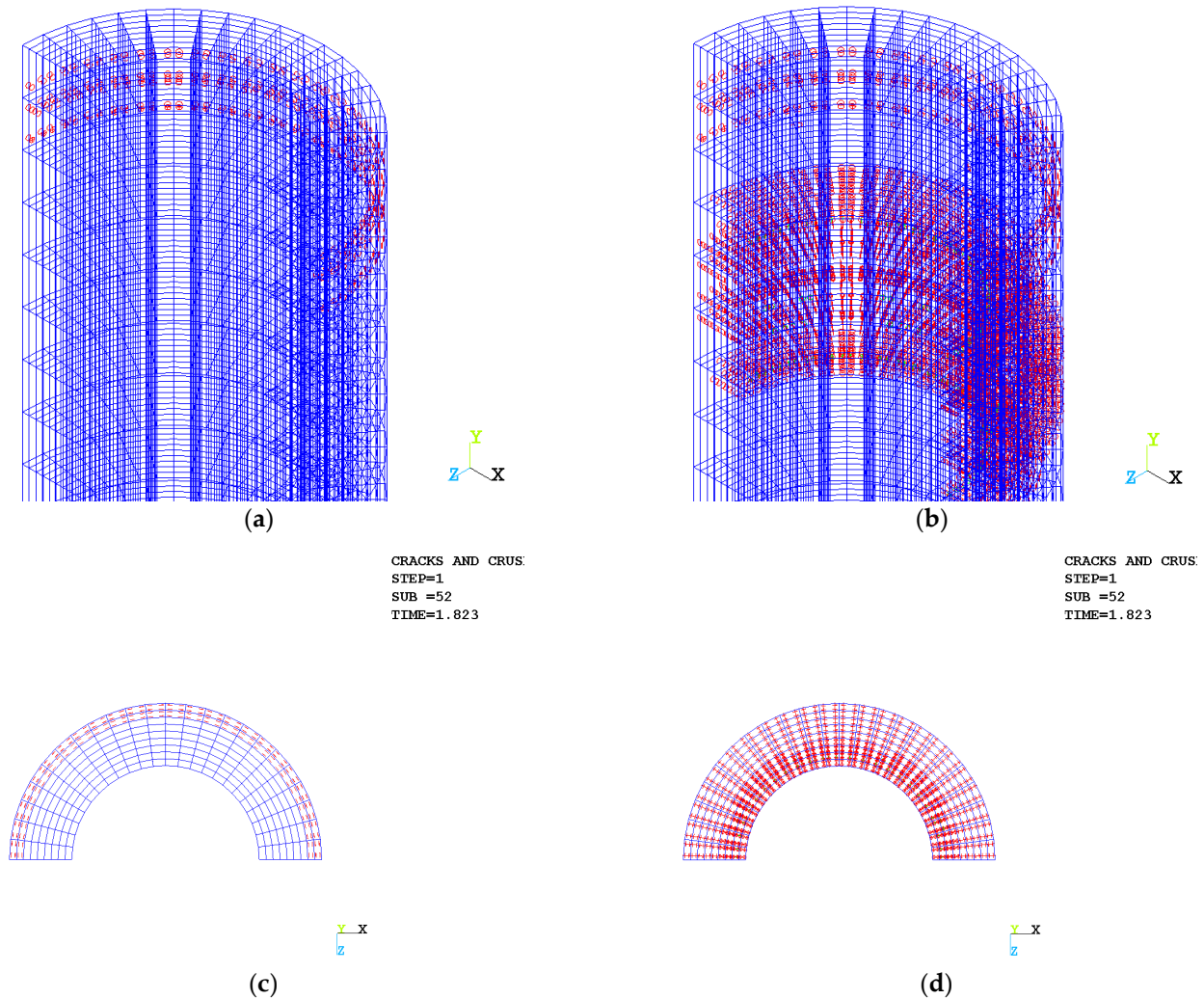

Figure 4. Cracking at the top support under compression without eccentricity for: (**a**,**c**) a homogeneous column in 3D and 2D; (**b**,**d**) a variotropic column in 3D and 2D with a force of 949 N.

As a result, the stress in the destroyed elements is close to zero, which can be seen in the inner layer of concrete of the variotropic column (Figure 3b). The homogeneous column continues to support the load. Some similarity of stress distribution can be observed between the body of a homogeneous column (Figure 3a) and two layers (outer and middle) of a variotropic one (Figure 3b), where the inner layer was turned off due to its destruction.

Figure 7a,b show the fields of equivalent stresses in reinforcement bars for homogeneous and three-layer columns, respectively. It can be seen that the reinforcing bars experience approximately the same compressive stresses, although the maximum stress values are localized in different zones.
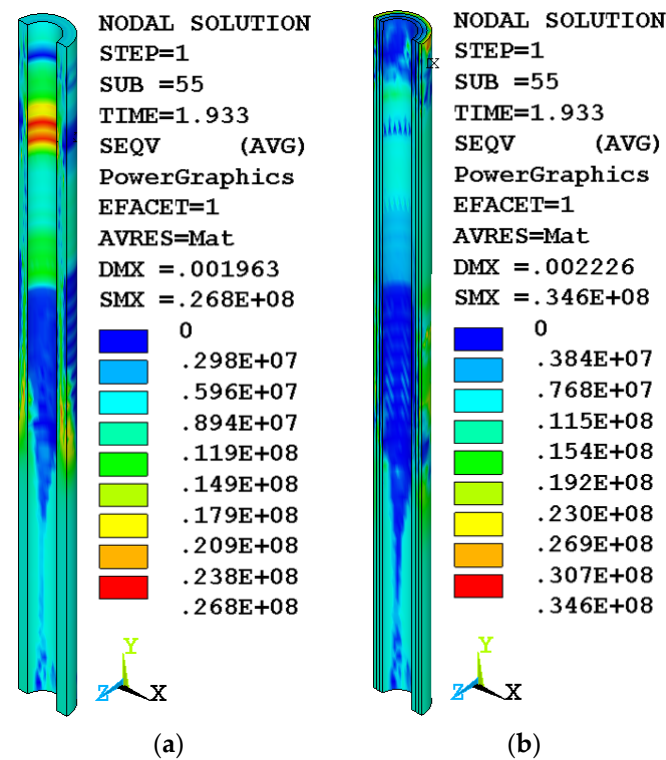
Figure 5. Equivalent stress fields in concrete in compression without eccentricity for (**a**) a homogeneous column; (**b**) variotropic in the area of critical failure.
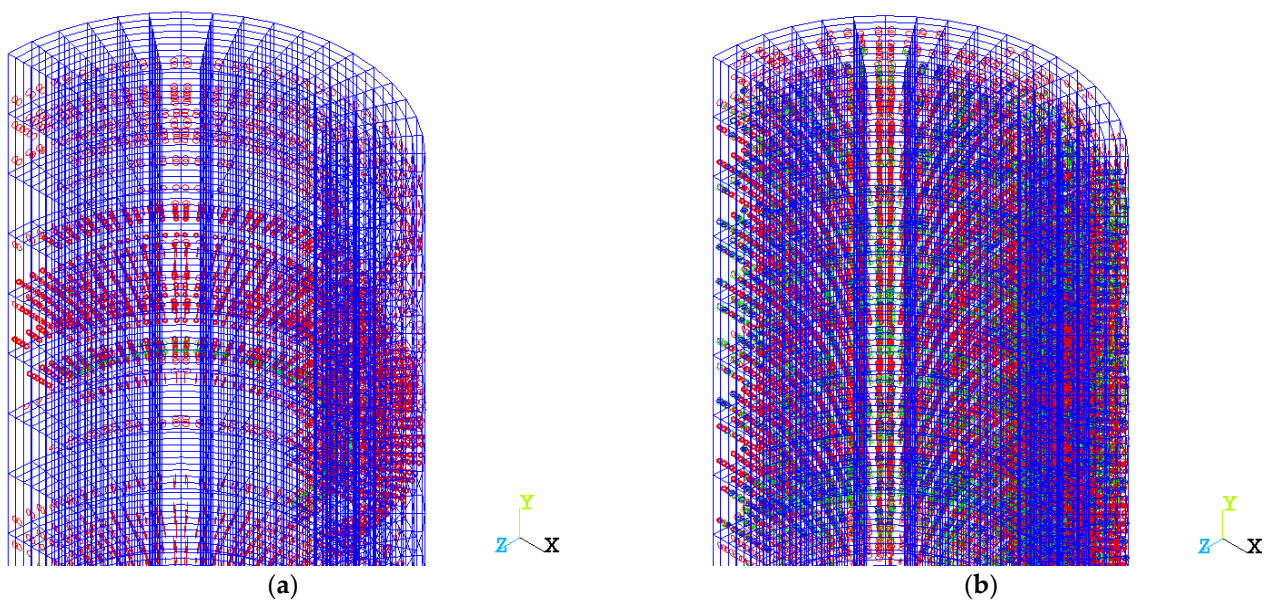
Figure 6. Cracking at the upper support during compression without eccentricity for (**a**) a homogeneous column and (**b**) a variotropic one in the area of critical failure.

3.2. Numerical Analysis of Compression of a Column with Eccentricity e = 24 mm

The results of solving the problems of loading a homogeneous column with an eccentricity *e* = 24 mm in the form of stress fields in concrete and reinforcement and schemes for the development of cracks in concrete are shown in Figures 8a, 9a, 10a and 11a, a three-layer column with the same eccentricity in Figures 8b, 9b, 10b and 11b.
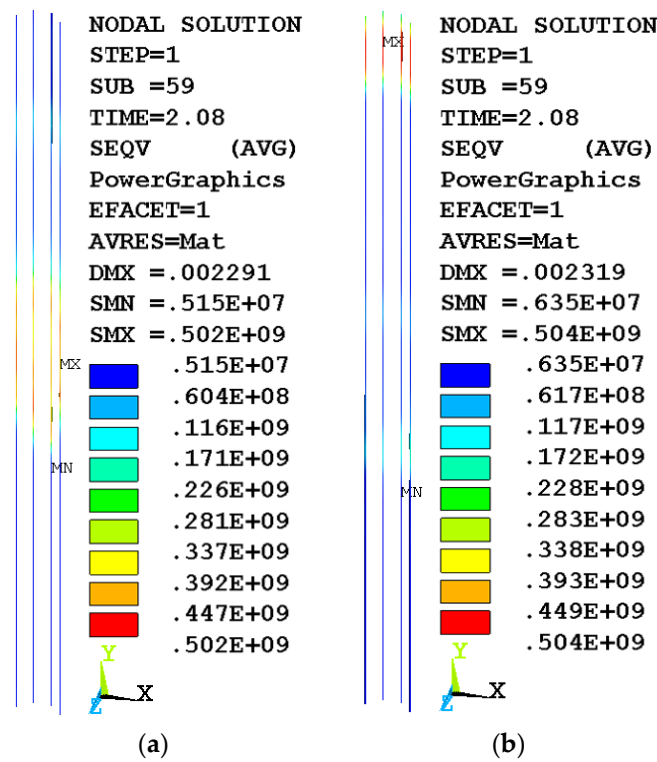
Figure 7. Fields of equivalent stresses in reinforcement under compression without eccentricity for (**a**) a homogeneous column (F = 112 kN); (**b**) a variotropic in the area of critical failure (F = 103 kN).
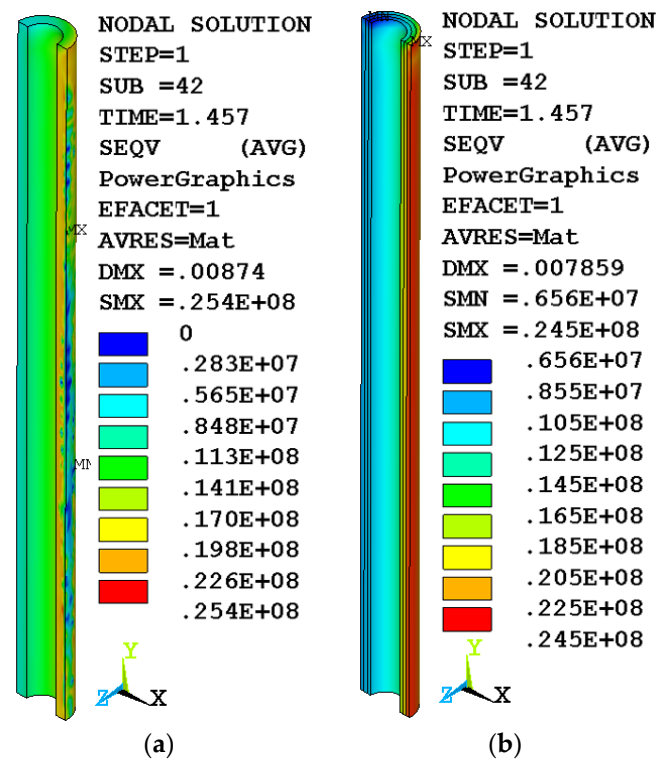

Figure 8. Fields of equivalent stresses in concrete under compression with eccentricity e = 24 mm for (**a**) homogeneous column (F = 686 kN); (**b**) variotropic (F = 710 kN).
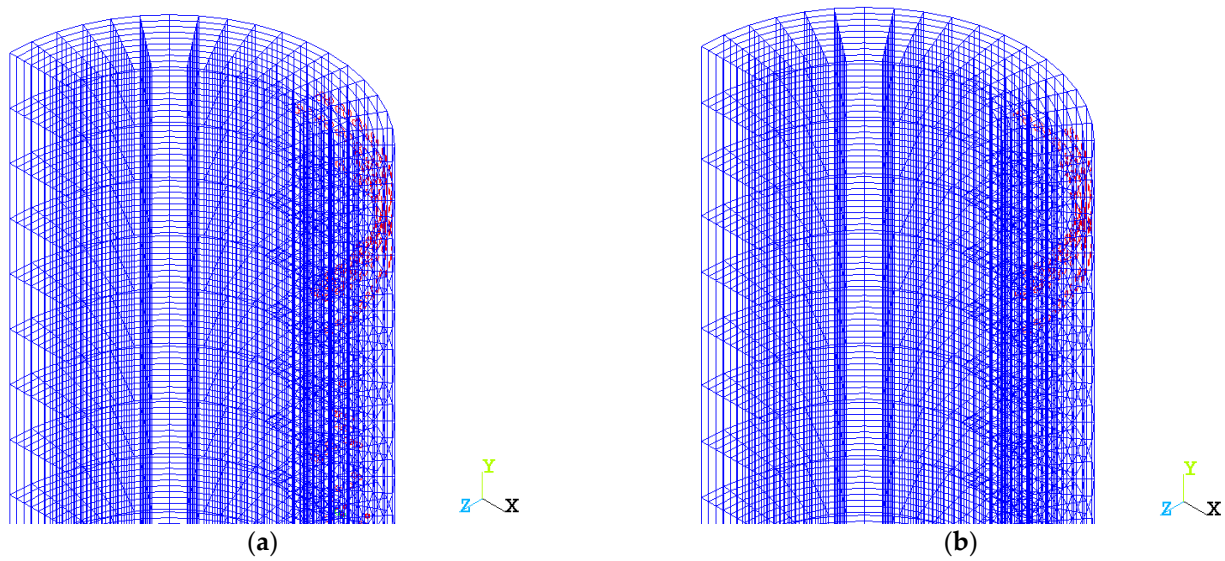
Figure 9. Crack formation near the upper support under compression with eccentricity *e* = 24 mm for (**a**) homogeneous column (F = 686 kN); (**b**) variotropic (F = 710 kN).
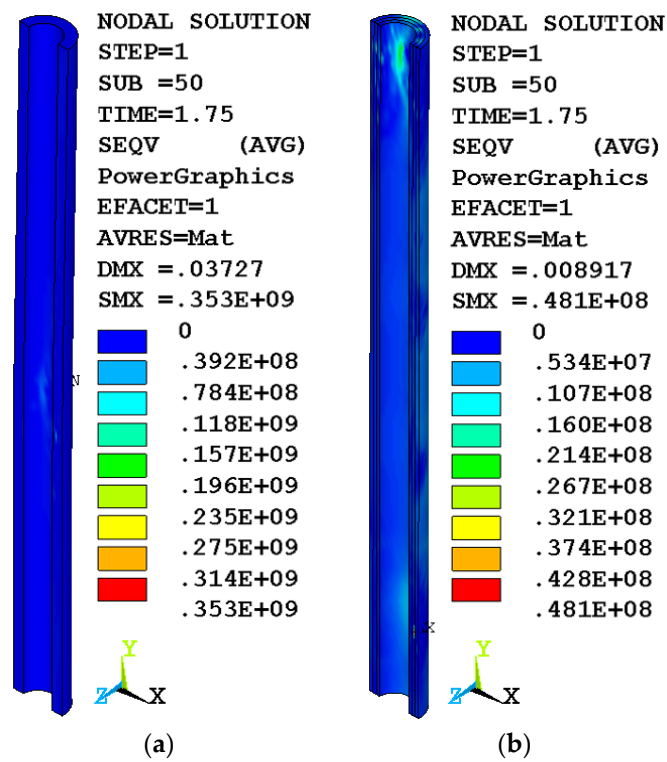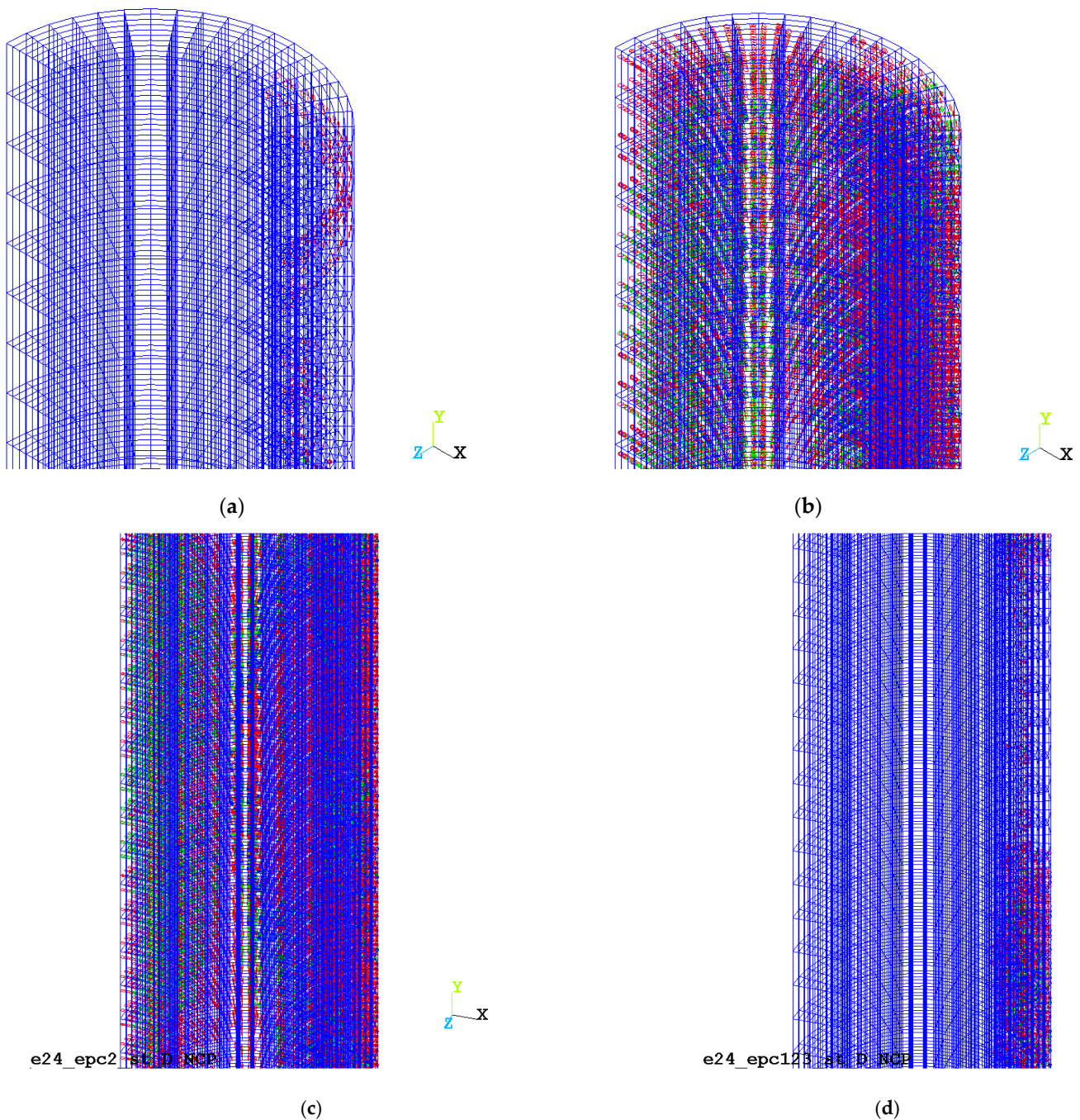

Figure 10. Fields of equivalent stresses in concrete under compression with eccentricity *e* = 24 mm for (**a**) homogeneous column and (**b**) variotropic (zone of supercritical destruction).

(**a**)

(**b**)

(**c**)

(**d**)

Figure 11. Compression cracking with eccentricity *e* = 24 mm for (**a**) a uniform column at the top support; (**b**) variotropic column at the top support; (**c**) a uniform column in the middle; (**d**) variotropic column in the middle part (supercritical fracture zone).

An analysis of stress fields and crack formation patterns shows a shift in the zone of the beginning of the destruction of a three-layer column compared to a homogeneous one both under central loading and eccentric.

Figure 8b shows that in a variotropic column, the outer layer perceives a large load and, due to increased strength, provides a large bearing capacity. Crack formation (Figure 9) is not as noticeable as with central compression and has a localized character.

The behavior of a variotropic column in the zone of supercritical failure shows a greater bearing capacity than a homogeneous one (Figure 10a,b). It can be seen that the

concrete of the homogeneous column has already been destroyed (the stress fields are close to 0), while the variotropic column is still resisting the load.

Analyzing Figure 8 and taking into account the results presented above, it becomes obvious that at the loading step 42 (with a displacement of the load application points by 1.46 mm), a homogeneous column resists with a force of 686 kN (Figure 8a), and a variotropic one with a force of 710 kN (Figure 8b). At the same time, the blue zone (blue spots) of stress fields on the surface of a homogeneous column (Figure 8a) indicates that the concrete sections in this area have already collapsed, and, consequently, the stresses in these sections have dropped to almost zero. Only the part of the concrete that survived at this stage, located closer to the center of the column, resists. Therefore, the stresses there are not equal to zero, but somewhere they reach the maximum values for this stage (in the range of 22.6–25.4 kPa). Figure 8b shows that the outer surface of the column is loaded to a value in the range from 22.5 to 24.5 MPa. This indicates that the material here still holds the load and has not collapsed. Thus, in the process of destruction, there is a constant redistribution of stresses along the sections of the columns, accompanied by an increase in these stresses in the surviving parts of the sections. Similar patterns can be seen in Figure 12.

(**a**)   (**b**)
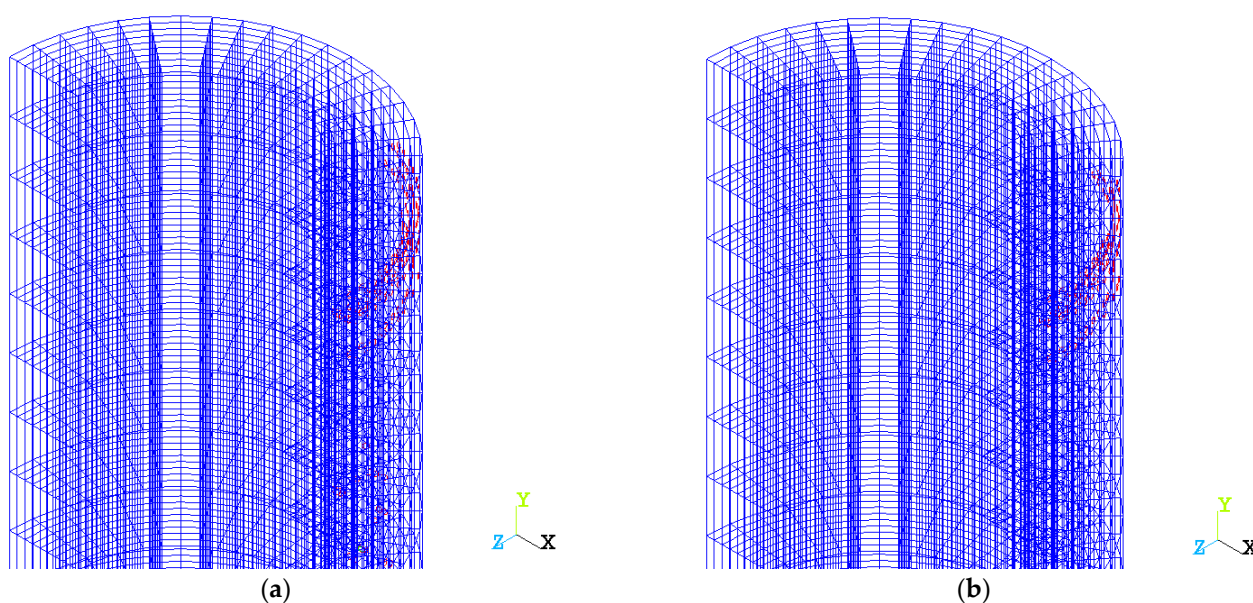
Figure 12. Cracking at the top support under compression with eccentricity *e* = 48 mm for (**a**) homogeneous column (F = 518 kN); (**b**) variotropic (F = 528 kN).

3.3. Numerical Analysis of Column Compression with Eccentricity e = 48 mm

The results of solving the problems of loading a homogeneous column with an eccentricity *e* = 48 mm in the form of stress fields in concrete and reinforcement and schemes for the development of cracks in concrete are shown in Figures 13a, 14a, 15a, 16a, 17a and 18a, a three-layer column with the same eccentricity—in Figures 13b, 14b, 15b, 16b, 17b and 18b.

As expected, eccentric loading of columns, both homogeneous and three-layer, occurs at a lower load than with central loading. The effect of heterogeneity is enhanced. A stronger outer layer resists eccentric compression bending better than a homogeneous column. With an eccentricity *e* = 48 mm, the decrease in strength, in comparison with the central compression, is about 47%. The difference in strength in terms of bearing capacity between homogeneous and three-layer structures, according to the calculation results, lies in the range from 4 to 6%.
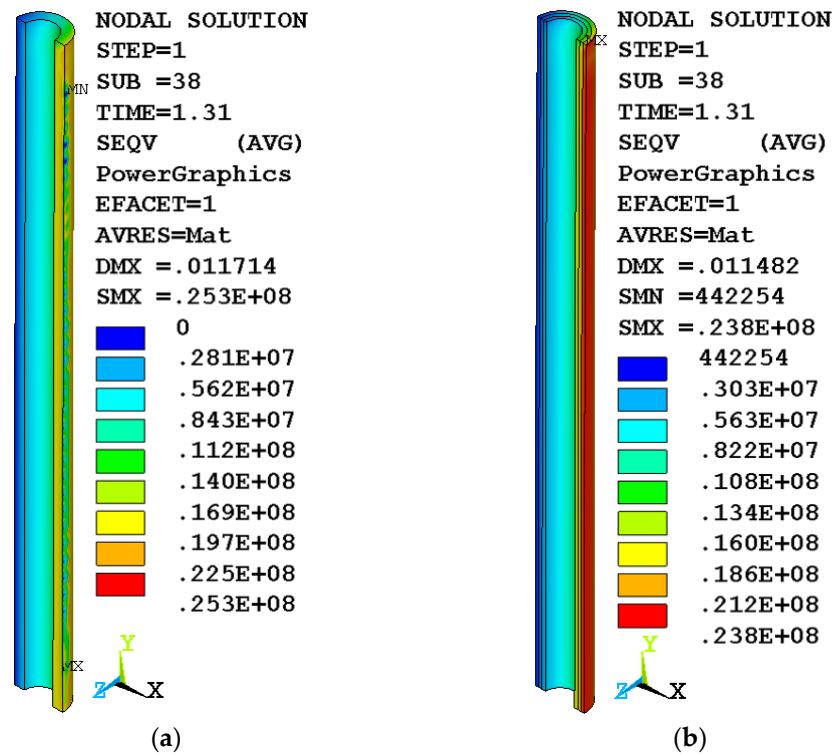
Figure 13. Fields of equivalent stresses in concrete under compression with eccentricity *e* = 48 mm for (**a**) a homogeneous column (F = 518 kN); (**b**) variotropic (F = 528 kN).
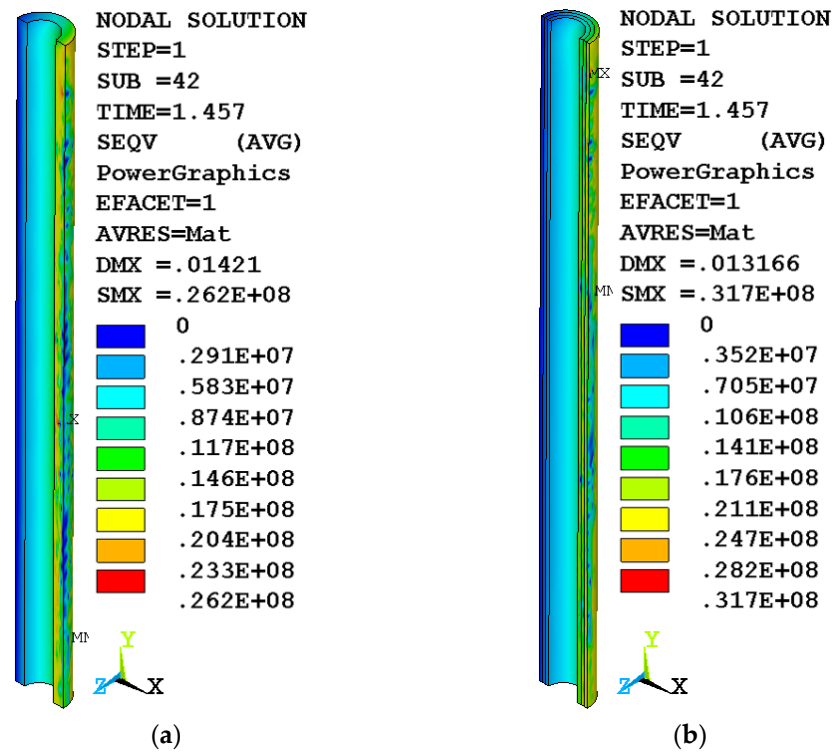

Figure 14. Fields of equivalent stresses in concrete under compression with eccentricity *e* = 48 mm for (**a**) a homogeneous column (F = 527 kN); (**b**) variotropic (F = 562 kN).
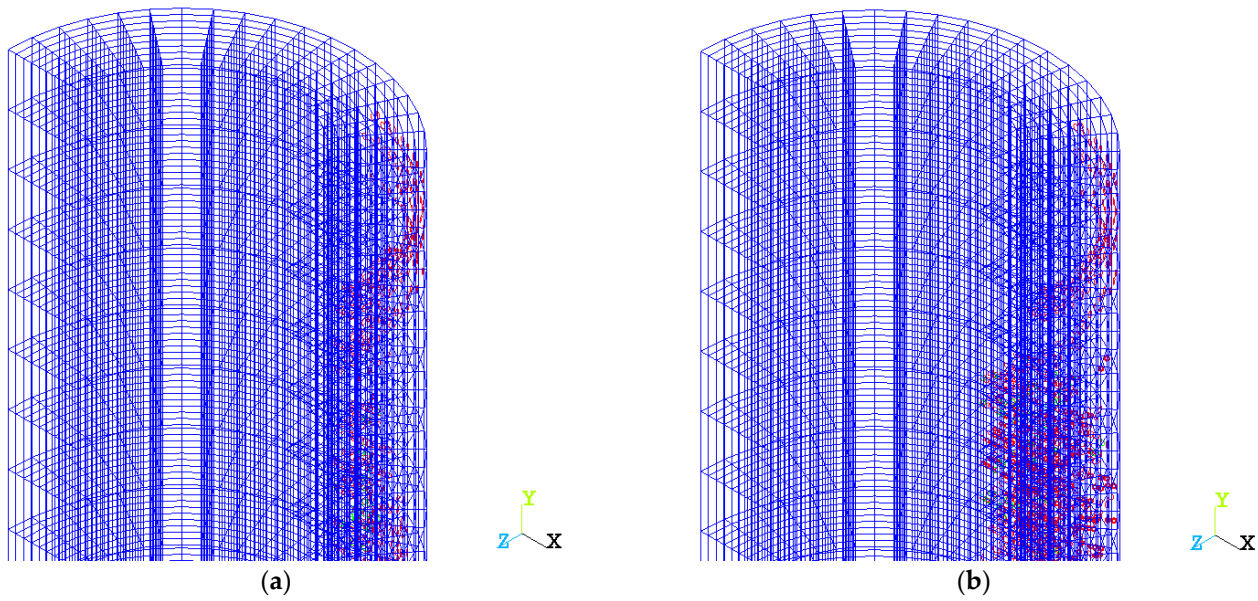
Figure 15. Cracking at the top support under compression with eccentricity *e* = 48 mm for (**a**) homogeneous column (F = 527 kN); (**b**) variotropic (F = 562 kN).
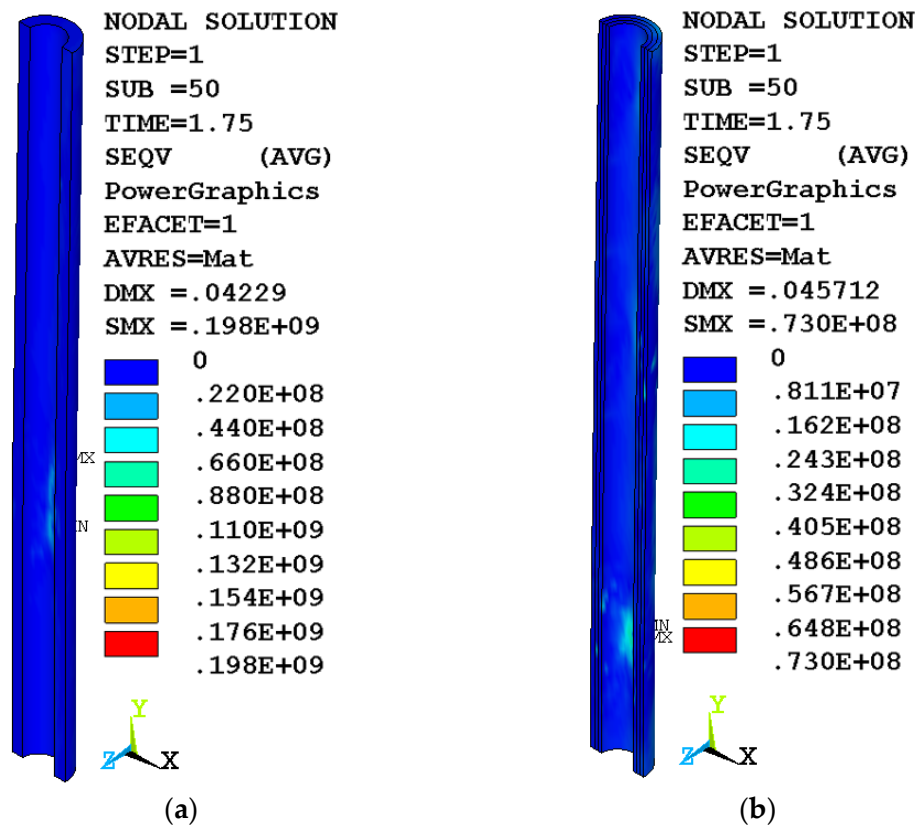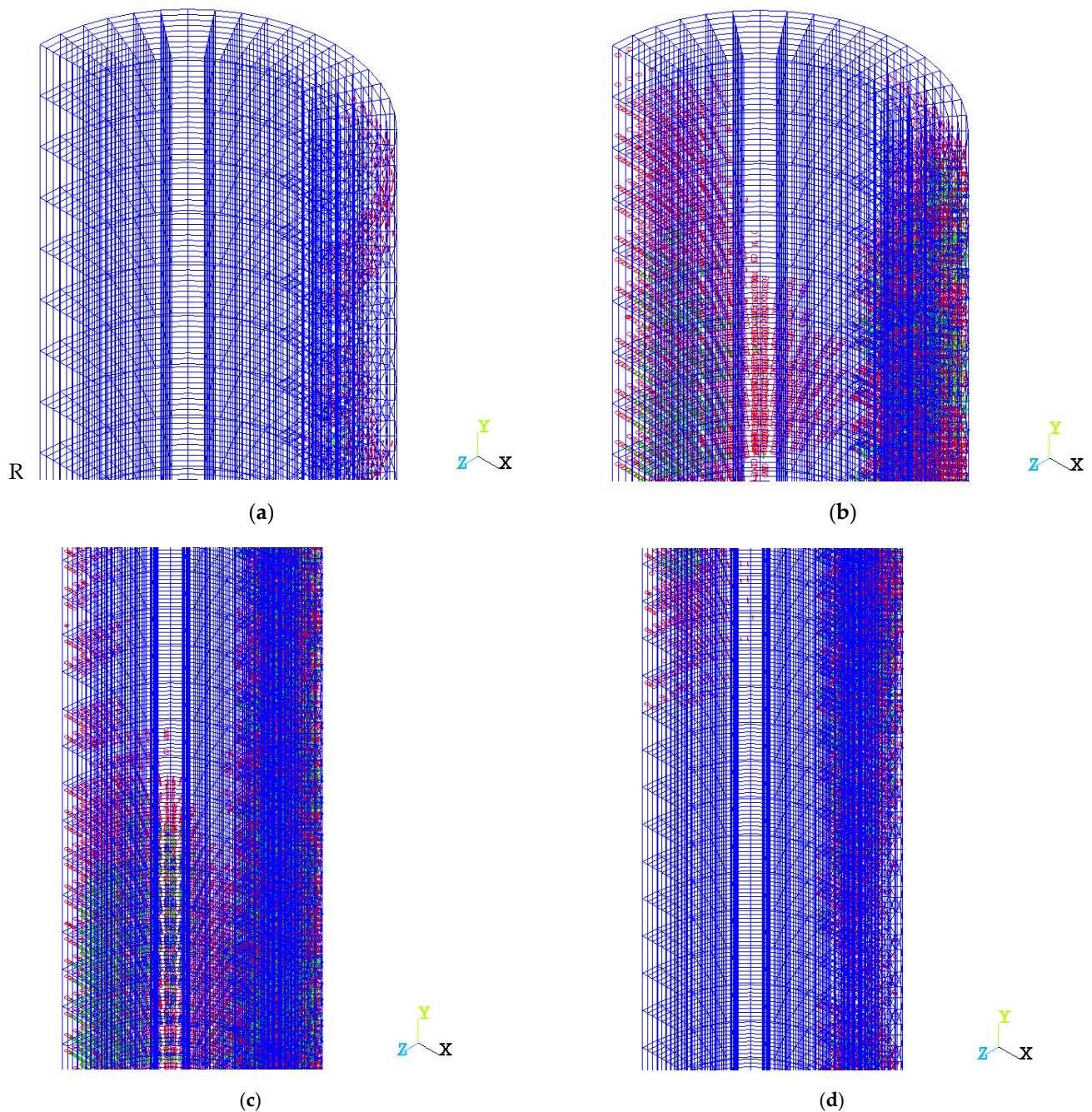

Figure 16. Fields of equivalent stresses in concrete under compression with eccentricity *e* = 48 mm for (**a**) homogeneous column and (**b**) variotropic (supercritical fracture zone).

Figure 17. Compression cracking with eccentricity *e* = 48 mm for (**a**) a uniform column at the top support; (**b**) variotropic column at the top support; (**c**) a uniform column in the middle; (**d**) variotropic column in the middle part (supercritical fracture zone).

In Figures 10 and 16, the main blue background (stresses close to zero) indicates the almost complete destruction of concrete and, consequently, the absence of stresses in it.

In Figures 5 and 14, blue spots can be observed in some areas (stresses close to zero). This may mean the destruction of concrete in these areas.

In Figures 13 and 14, the areas of continuous blue color only indicate the current level of stresses in these zones until the moment of their destruction.

In general, an increase in eccentricity leads to a decrease in the bearing capacity (Figure 2), but the difference between the bearing capacity of homogeneous and variotropic columns increases. The greater the eccentricity, the better the variotropic columns work

than the homogeneous ones, although in comparison with the central compression, the bearing capacity decreases.
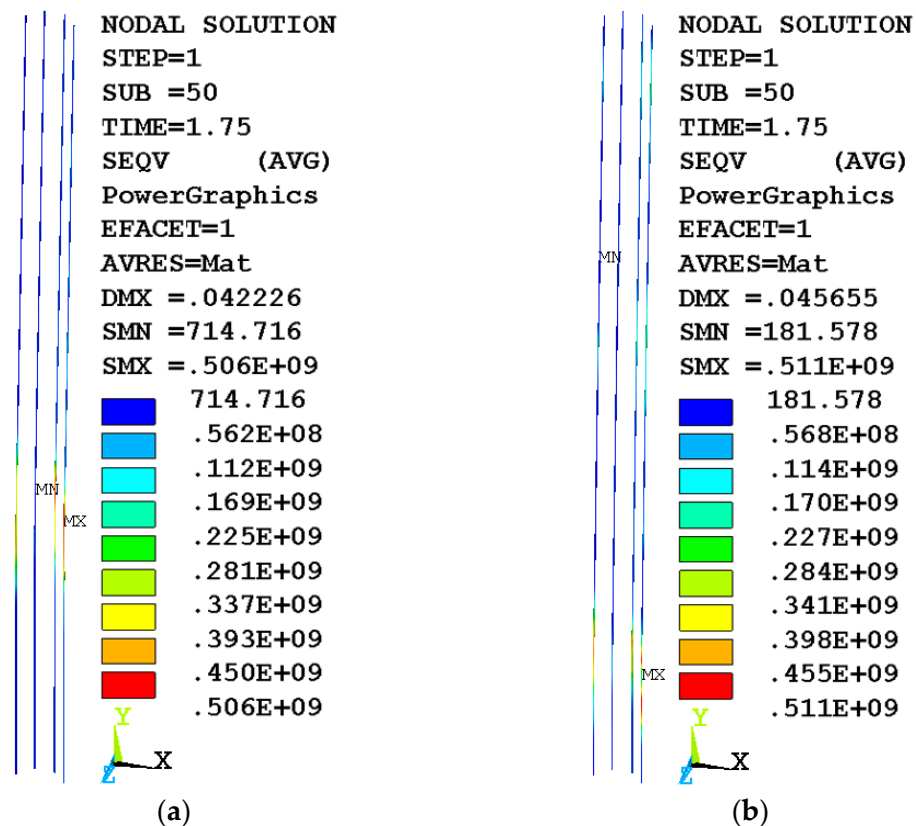
Figure 18. Fields of equivalent stresses in reinforcement under compression with eccentricity *e* = 48 mm for (**a**) homogeneous column and (**b**) variotropic (supercritical fracture zone).

An analysis of the stress–strain state of the considered columns shows that the results largely correspond to the data obtained by other researchers. Thus, it can be seen that, as in [72], the column characteristically bends during deformation, and in the compressed region, a characteristic buckling of the material occurs with the formation of folds and subsequent destruction. However, unlike a steel pipe [72], the plastic deformation of concrete is less noticeable and rapid cracking occurs [26]. Indeed, plastic deformation of concrete is possible within much smaller limits due to the fragility of the nature of the destruction of this material. The steel pipe exhibits a large degree of plastic deformation due to the properties of the steel. In this investigation, there is a variability of concrete, that is, its heterogeneity in cross section. Therefore, in the case of the occurrence of eccentricity, there is some redistribution of the nature of the deformation, and hence the nature of its plasticity. The work of the variotropic structure under load changes precisely on concrete, since the properties of concrete become heterogeneous. Thus, a change in the nature of cracking occurs during plastic deformations.

The heterogeneity of variotropic concrete, as well as the conditions of rigid adhesion of concrete along the upper boundary of the column, change the stress–strain state and redistribute the zones of crack initiation. It can be seen (Figure 13a,b) that in a variotropic column, cracking begins in the upper part of the column, and in a homogeneous column, in the middle (Figure 17c,d). A similar character of deformation is observed in [73,74] during experimental studies.

The results obtained in [75,76] are qualitatively and quantitatively similar to the results of this article. As in this article, the nature of the failure under an eccentrically applied load leads to distortion and local buckling of the column. However, the inhomogeneity of the column material considered in this article leads to a redistribution of stresses and a

shift in the zone of the beginning of destruction. These two works agree in an interesting way with our results. For example, the authors of [75] in their work were guided by a recipe-technological method—additional dispersed reinforcement of the column concrete with the help of fiber. Attention is drawn to the constructive solution of the column—this is a steel–concrete version. Thus, the authors of [75], having applied an integrated design and technological approach, managed to achieve an increase in the bearing capacity of about 200%. In the same article, an effect was revealed that is the release of a hidden resource at a certain eccentricity, which amounted to about 6%. At the same time, no additional techniques were used in this study. In addition, the work [76] seems interesting. Its authors found that "eccentricity has the greatest influence on the mechanical properties of the sample under shearing pressure, followed by the direction of the eccentricity, and finally the length of the sample. The influence of the eccentricity and the direction of the eccentricity on the mechanical properties of the sample under bias pressure is more significant than the length of the sample". This result vividly characterizes columns with an interesting design solution—a T-shaped configuration. In the same article, columns with an annular configuration are also investigated, in addition to being variotropic in their cross section. In the same article, as well as the authors of [76], the nature of the influence of eccentricity is established, which helps to better understand and apply operational nuances in such non-standard structures and buildings.

4. Conclusions

The problem of central and eccentric compression of homogeneous and variotropic columns is considered for various types of eccentricity e/r = 0; 0.16; 0.32 (or 0; 24 mm; 48 mm). The variotropic column is represented by a three-layer material, in which the inner layer has the lowest strength, the middle layer has the strength equal to the strength of a homogeneous column, and the outer layer has the highest strength. An analysis of the stress–strain state of a variotropic column in comparison with a homogeneous one shows a significant change in the bearing capacity and characteristic zones of crack initiation.

(1) It is shown that under central compression, a homogeneous column has a 3.6% higher bearing capacity than a variotropic one.

(2) Eccentric compression with eccentricity e/r = 0.16; 0.32 changes the stress–strain state of the column and the variotropic column has a 5.5% and 6.2% higher bearing capacity, respectively, than a homogeneous one.

(3) It is shown that the nature of the stress–strain state changes and the zone of the beginning of destruction near the variotropic column shifts upward to the zone of application of the load.

(4) The obtained results show that the variotropic column design has an advantage in the bearing capacity of eccentrically compressed columns and can be implemented in practice.

(5) The revealed positive effect of the variotropy of the concrete structure of eccentrically compressed reinforced concrete columns develops the previously known theory of the advantages of such columns in the case of central compression. This relationship proves the high efficiency and the possibility of using variotropic columns in technically complex structures with increased responsibility.

(6) The research recommendation is to propose to develop the study of the work of variotropic structures in non-trivial problems. In particular, these are other types of stress–strain states other than the compressed state, other types of compressed structures in terms of geometry and design solutions, and the continuation of work on studying the effect of eccentricity on them.

(7) Prospects for the development of research lie in the direction of studying the relationship between the geometric and design parameters of variotropic columns and their bearing capacity under central and eccentric loading. The scope of future work is to assess the effect of the heterogeneity of the structure of variotropic reinforced concrete beams on their performance under dynamic loads.

References

1. Aksoylu, C.; Özkılıç, Y.O.; Arslan, M.H. Mechanical Steel Stitches: An innovative approach for strengthening shear deficiency in undamaged reinforced concrete beams. *Buildings* **2022**, *12*, 1501. [CrossRef]
2. Zhang, Z.; Li, W.; Yang, J. Analysis of stochastic process to model safety risk in construction industry. *J. Civ. Eng. Manag.* **2021**, *27*, 87–99. [CrossRef]
3. Gemi, L.; Alsdudi, M.; Aksoylu, C.; Yazman, Ş.; Özkılıç, Y.O.; Arslan, M.H. Optimum amount of CFRP for strengthening shear deficient reinforced concrete beams. In *Steel and Composite Structures*; Techno-Press: Daejeon, Republic of Korea, 2022.
4. Korkmaz, H.H.; Dere, Y.; Özkılıç, Y.O.; Bozkurt, M.B.; Ecemiş, A.S.; Özdoner, N. Excessive snow induced steel roof failures in Turkey. *Eng. Fail. Anal.* **2022**, *141*, 106661. [CrossRef]
5. Abdal, S.; Mansour, W.; Agwa, I.; Nasr, M.; Abadel, A.; Özkılıç, Y.O.; Akeed, M.H. Application of ul-tra-high-performance concrete in bridge engineering: Current status, limitations, challenges, and future prospects. *Buildings* **2023**, *13*, 185. [CrossRef]
6. Ilyas, M.; Ahmad, A.; Riaz, A.; Khan, F.A.; Sher, S.; Waseem, M.; Ali, S.Z.; Badrashi, Y.I.; Waqas, H.A.; Seitz, H.; et al. Review of Modeling Techniques for Analysis and Assessment of RC Beam–Column Joints Subjected to Seismic Loads. *Materials* **2022**, *15*, 7448. [CrossRef] [PubMed]
7. Mina, A.L.; Petrou, M.F.; Trezos, K.G. Resistance of an Optimized Ultra-High Performance Fiber Reinforced Concrete to Projectile Impact. *Buildings* **2021**, *11*, 63. [CrossRef]
8. Huang, H.; Guo, M.; Zhang, W.; Zeng, J.; Yang, K.; Bai, H. Numerical investigation on the bearing capacity of RC columns strengthened by HPFL-BSP under combined loadings. *J. Build. Eng.* **2021**, *39*, 102266. [CrossRef]
9. Özkılıç, Y.O.; Aksoylu, C.; Arslan, M.H. Numerical evaluation of effects of shear span, stirrup spacing and angle of stirrup on reinforced concrete beam behaviour. *Struct. Eng. Mech.* **2021**, *79*, 309–326.
10. Li, J.; Chen, M.; Li, Z. Improved soil–structure interaction model considering time-lag effect. *Comput. Geotech.* **2022**, *148*, 104835. [CrossRef]
11. Özkılıç, Y.O.; Karalar, M.; Aksoylu, C.; Beskopylny, A.N.; Stel'makh, S.A.; Shcherban, E.M.; Qaidi, S.; Pereira, I.d.S.; Monteiro, S.N.; Azevedo, A.R. Shear performance of reinforced expansive concrete beams utilizing aluminium waste. *J. Mater. Res. Technol.* **2023**, *24*, 5433–5448. [CrossRef]
12. Huang, H.; Huang, M.; Zhang, W.; Guo, M.; Liu, B. Progressive collapse of multistory 3D reinforced concrete frame structures after the loss of an edge column. *Struct. Infrastruct. Eng.* **2022**, *18*, 249–265. [CrossRef]
13. Shafighfard, T.; Bagherzadeh, F.; Rizi, R.A.; Yoo, D.-Y. Data-driven compressive strength prediction of steel fiber reinforced concrete (SFRC) subjected to elevated temperatures using stacked machine learning algorithms. *J. Mater. Res. Technol.* **2022**, *21*, 3777–3794. [CrossRef]
14. Kos, Z.; Klymenko, Y.; Crnoja, A.; Grynyova, I. Calculation Model for Estimation of Residual Bearing Capacity of Damaged Reinforced Concrete Slender Columns. *Appl. Sci.* **2022**, *12*, 7430. [CrossRef]
15. Evtushenko, S.I.; Petrov, I.A.; Shutova, M.N.; Chernykhovsky, B.A. Bearing capacity of eccentrically compressed bisteel columns. *Mag. Civ. Eng.* **2021**, *2*, 10201. [CrossRef]
16. Fang, B.; Hu, Z.; Shi, T.; Liu, Y.; Wang, X.; Yang, D.; Zhu, K.; Zhao, X.; Zhao, Z. Research progress on the properties and applications of magnesium phosphate cement. *Ceram. Int.* **2022**, *49*, 4001–4016. [CrossRef]
17. Shi, T.; Liu, Y.; Zhao, X.; Wang, J.; Zhao, Z.; Corr, D.J.; Shah, S.P. Study on mechanical properties of the interfacial transition zone in carbon nanofiber-reinforced cement mortar based on the PeakForce tapping mode of atomic force microscope. *J. Build. Eng.* **2022**, *61*, 105248. [CrossRef]
18. Shi, T.; Liu, Y.; Hu, Z.; Cen, M.; Zeng, C.; Xu, J.; Zhao, Z. Deformation Performance and Fracture Toughness of Carbon Nanofiber Modified Cement-Based Materials. *ACI Mater. J.* **2022**, *119*, 119–128. [CrossRef]
19. Wang, M.; Yang, X.; Wang, W. Establishing a 3D aggregates database from X-ray CT scans of bulk concrete. *Constr. Build. Mater.* **2022**, *315*, 125740. [CrossRef]

20. Zhou, S.; Lu, C.; Zhu, X.; Li, F. Preparation and Characterization of High-Strength Geopolymer Based on BH-1 Lunar Soil Simulant with Low Alkali Content. *Engineering* **2021**, *7*, 1631–1645. [CrossRef]

21. Huang, H.; Li, M.; Zhang, W.; Yuan, Y. Seismic behavior of a friction-type artificial plastic hinge for the precast beam–column connection. *Arch. Civ. Mech. Eng.* **2022**, *22*, 201. [CrossRef]

22. Zhai, S.-Y.; Lyu, Y.-F.; Cao, K.; Li, G.-Q.; Wang, W.-Y.; Chen, C. Seismic behavior of an innovative bolted connection with dual-slot hole for modular steel buildings. *Eng. Struct.* **2023**, *279*, 115619. [CrossRef]

23. Huang, Y.; Zhang, W.; Liu, X. Assessment of Diagonal Macrocrack-Induced Debonding Mechanisms in FRP-Strengthened RC Beams. *J. Compos. Constr.* **2022**, *26*, 4022056. [CrossRef]

24. Ghasemi, M.; Zhang, C.; Khorshidi, H.; Zhu, L.; Hsiao, P.-C. Seismic upgrading of existing RC frames with displacement-restraint cable bracing. *Eng. Struct.* **2023**, *282*, 115764. [CrossRef]

25. Huang, H.; Yao, Y.; Liang, C.; Ye, Y. Experimental study on cyclic performance of steel-hollow core partially encased composite spliced frame beam. *Soil Dyn. Earthq. Eng.* **2022**, *163*, 107499. [CrossRef]

26. Beskopylny, A.N.; Meskhi, B.; Stel'makh, S.A.; Shcherban', E.M.; Mailyan, L.R.; Veremeenko, A.; Akopyan, V.; Shilov, A.V.; Chernil'nik, A.; Beskopylny, N. Numerical Simulation of the Bearing Capacity of Variotropic Short Concrete Beams Reinforced with Polymer Composite Reinforcing Bars. *Polymers* **2022**, *14*, 3051. [CrossRef]

27. Beskopylny, A.; Stel'makh, S.A.; Shcherban', E.M.; Mailyan, L.R.; Meskhi, B. Nano modifying additive micro silica influence on integral and differential characteristics of vibrocentrifuged concrete. *J. Build. Eng.* **2022**, *51*, 104235. [CrossRef]

28. Beskopylny, A.N.; Shcherban', E.M.; Stel'makh, S.A.; Mailyan, L.R.; Meskhi, B.; Evtushenko, A.; Varavka, V.; Beskopylny, N. Nano-Modified Vibrocentrifuged Concrete with Granulated Blast Slag: The Relationship between Mechanical Properties and Micro-Structural Analysis. *Materials* **2022**, *15*, 4254. [CrossRef] [PubMed]

29. Šapalas, A.; Mudrov, A. Analysing the Confinement Effect in Hollow Core Steel-Concrete Composite Columns under Axial Compression. *Materials* **2021**, *14*, 6046. [CrossRef] [PubMed]

30. Wang, J.; Duan, Y.; Wang, Y.; Wang, X.; Liu, Q. Analysis and Modification of Methods for Calculating Axial Load Capacity of High-Strength Steel-Reinforced Concrete Composite Columns. *Materials* **2021**, *14*, 6860. [CrossRef]

31. Won, D.; Kim, S.; Seo, J.; Kang, Y.-J. Experimental Study of Composite Hollow RC Column under Uniaxial Compressive Load. *Appl. Sci.* **2019**, *9*, 373. [CrossRef]

32. Cai, H.; Yan, Y. UHPC-Filled Rectangular Steel Tubular Beam–Column: Numerical Study and Design. *Buildings* **2022**, *12*, 1882. [CrossRef]

33. Cao, B.; Xie, M.; Huang, B.; Hu, G.; Wang, J. Axial Compression Performance of Precast Circular Semi-Continuous Concrete-Filled Steel Tube Columns: Finite Element Analysis and Theoretical Modeling. *Buildings* **2023**, *13*, 284. [CrossRef]

34. Sarir, P.; Jiang, H.; Asteris, P.G.; Formisano, A.; Armaghani, D.J. Iterative Finite Element Analysis of Concrete-Filled Steel Tube Columns Subjected to Axial Compression. *Buildings* **2022**, *12*, 2071. [CrossRef]

35. Bai, W.; Li, Y.; Ji, J.; Liu, Y.; Zhang, L.; Wang, R.; Jiang, L.; He, L. Axial Compression Behavior of Symmetrical Full-Scale Concrete Filled Double Skin Steel Tube Stub Columns. *Symmetry* **2022**, *14*, 223. [CrossRef]

36. Wang, J.; Wang, X.; Duan, Y.; Su, Y.; Yi, X. The Investigation on Mechanical Performances of High-Strength Steel Reinforced Concrete Composite Short Columns under Axial Load. *Materials* **2022**, *15*, 329. [CrossRef]

37. Miao, K.; Wei, Y.; Zhang, X.; Zheng, K.; Dong, F. Performance of Circular Concrete-Filled FRP-Grooved Steel Composite Tube Columns under Axial Compression. *Polymers* **2021**, *13*, 3638. [CrossRef]

38. Zhang, Z.; Wang, J.; Sun, Q.; Tian, P.; Wang, J.; Wu, Y.; Li, Y. Experimental and Numerical Study of the Behavior of Concrete-Filled High-Strength Steel Tube Columns with Large D/t Ratio under Axial Compression. *Buildings* **2022**, *12*, 1953. [CrossRef]

39. Veerapandian, V.; Pandulu, G.; Jayaseelan, R.; Sathish Kumar, V.; Murali, G.; Vatin, N.I. Numerical Modelling of Geopolymer Concrete In-Filled Fibre-Reinforced Polymer Composite Columns Subjected to Axial Compression Loading. *Materials* **2022**, *15*, 3390. [CrossRef]

40. Wang, W.-D.; Ji, S.-H.; Shi, Y.-L. Experimental and numerical investigations on concrete-filled double-tubular slender columns under axial and eccentric loading. *J. Constr. Steel Res.* **2023**, *201*, 107714. [CrossRef]

41. Abadel, A.A.; Khan, M.I.; Masmoudi, R. Experimental and numerical study of compressive behavior of axially loaded circular ultra-high-performance concrete-filled tube columns. *Case Stud. Constr. Mater.* **2022**, *17*, e01376. [CrossRef]

42. Havlásek, P. Numerical modeling of axially compressed circular concrete columns. *Eng. Struct.* **2021**, *227*, 111445. [CrossRef]

43. Zhang, X.; Ding, Y.; Wang, X.; Sun, L. Study on Eccentric Compressive Behavior of Concrete Columns Reinforced with NPR735 High-Strength Steel Bars. *Buildings* **2023**, *13*, 188. [CrossRef]

44. Wang, X.; Li, Y.; Zhao, Y.; Wei, Y.; Fan, J. Compressive Performance of RC Columns Strengthened with High-Strength Stainless Steel Wire Mesh-ECC under Small Eccentric Compression Load. *Buildings* **2022**, *12*, 1628. [CrossRef]

45. Chepurnenko, A.; Lipovich, A.; Beskopylny, A.N.; Meskhi, B. Reinforced Concrete Columns with Local Prestressing Rebars: A Calculation Theory and an Experimental Study. *Buildings* **2022**, *12*, 1152. [CrossRef]

46. Cassese, P.; Menna, C.; Occhiuzzi, A.; Asprone, D. Experimental Behavior of Existing RC Columns Strengthened with HPFRC Jacket under Concentric and Eccentric Compressive Load. *Buildings* **2021**, *11*, 521. [CrossRef]

47. Li, Q.; Kuang, Y.; Guo, W.; Zhang, Y. Experimental Research on Mechanical Performance of SSRC Columns under Eccentric Compression. *Appl. Sci.* **2020**, *10*, 5629. [CrossRef]

48. Hou, Y.; Cao, S.; Ni, X.; Li, Y. Research on Concrete Columns Reinforced with New Developed High-Strength Steel under Eccentric Loading. *Materials* **2019**, *12*, 2139. [CrossRef] [PubMed]

49. Li, C.; Geng, H.; Deng, C.; Li, B.; Zhao, S. Experimental Investigation on Columns of Steel Fiber Reinforced Concrete with Recycled Aggregates under Large Eccentric Compression Load. *Materials* **2019**, *12*, 445. [CrossRef] [PubMed]

50. Berardi, V.P.; Mancusi, G. Time-Dependent Behavior of Reinforced Polymer Concrete Columns under Eccentric Axial Loading. *Materials* **2012**, *5*, 2342–2352. [CrossRef]

51. Polskoy, P.P.; Mailyan, D.; Beskopylny, A.N.; Meskhi, B.; Shilov, A.V.; Umarov, A. Strength of Compressed Reinforced Concrete Elements Reinforced with CFRP at Different Load Application Eccentricity. *Polymers* **2023**, *15*, 26. [CrossRef]

52. Wysmulski, P. Load Eccentricity of Compressed Composite Z-Columns in Non-Linear State. *Materials* **2022**, *15*, 7631. [CrossRef] [PubMed]

53. Li, X.; Xie, H.; Yan, M.; Gou, H.; Zhao, G.; Bao, Y. Eccentric Compressive Behavior of Reinforced Concrete Columns Strengthened Using Steel Mesh Reinforced Resin Concrete. *Appl. Sci.* **2018**, *8*, 1827. [CrossRef]

54. Hu, B.; Wang, J.-G.; Li, G.-Q. Numerical simulation and strength models of FRP-wrapped reinforced concrete columns under eccentric loading. *Constr. Build. Mater.* **2011**, *25*, 2751–2763. [CrossRef]

55. Ma, Y.-X.; Zhao, O.; Tan, K.H. Experimental and numerical studies of concrete-encased concrete-filled steel tube stub columns under uniaxial and biaxial eccentric compression. *Eng. Struct.* **2021**, *232*, 111796. [CrossRef]

56. Li, G.-C.; Chen, B.-W.; Yang, Z.-J.; Liu, Y.-P.; Feng, Y.-H. Experimental and numerical behavior of eccentrically loaded square concrete-filled steel tubular long columns made of high-strength steel and concrete. *Thin-Walled Struct.* **2021**, *159*, 107289. [CrossRef]

57. Ahmed, M.; Liang, Q.Q.; Patel, V.I.; Hadi, M.N.S. Experimental and numerical studies of square concrete-filled double steel tubular short columns under eccentric loading. *Eng. Struct.* **2019**, *197*, 109419. [CrossRef]

58. Nie, G.J.; Batra, R.C. Material tailoring and analysis of functionally graded isotropic and incompressible linear elastic hollow cylinders. *Compos. Struct.* **2010**, *92*, 265–274. [CrossRef]

59. Abdelkarim, O.I.; ElGawady, M.A. Dynamic and Static Behavior of Hollow-Core FRP-Concrete-Steel and Reinforced Concrete Bridge Columns under Vehicle Collision. *Polymers* **2016**, *8*, 432. [CrossRef]

60. Chepurnenko, A.; Litvinov, S.; Meskhi, B.; Beskopylny, A. Optimization of Thick-Walled Viscoelastic Hollow Polymer Cylinders by Artificial Heterogeneity Creation: Theoretical Aspects. *Polymers* **2021**, *13*, 2408. [CrossRef]

61. Wei, Y.; Xu, Y.; Wang, G.; Cheng, X.; Li, G. Influence of the Cross-Sectional Shape and Corner Radius on the Compressive Behaviour of Concrete Columns Confined by FRP and Stirrups. *Polymers* **2022**, *14*, 341. [CrossRef]

62. Li, D.-C.; Xu, C.; Cui, Z.-D.; Chen, J.-M.; Xu, X.-Q.; Zhang, T.-T.; Zhang, Z.-W.; Song, G. Mechanical Properties of Functionally Graded Concrete Lining for Deep Underground Structures. *Adv. Civ. Eng.* **2022**, *2022*, 2363989. [CrossRef]

63. Skrivanek, J.; Holec, P.; Batka, O.; Bilek, M.; Pokorny, P. Optimization of the Spinneret Rotation Speed and Airflow Parameters for the Nozzleless Forcespinning of a Polymer Solution. *Polymers* **2022**, *14*, 1042. [CrossRef] [PubMed]

64. Chen, T.-H.; Huang, S.-Y.; Huang, S.-Y.; Lin, J.-D.; Huang, B.-Y.; Kuo, C.-T. Improvement of the Centrifugal Force in Gravity Driven Method for the Fabrication of Highly Ordered and Submillimeter-Thick Colloidal Crystal. *Polymers* **2021**, *13*, 692. [CrossRef] [PubMed]

65. Feng, Z.; Hu, H.; Dong, Y.; Wang, F.; Jia, M.; Zhao, Y.; He, J. Effect of Steel Casing on Vertical Bearing Characteristics of Steel Tube-Reinforced Concrete Piles in Loess Area. *Appl. Sci.* **2019**, *9*, 2874. [CrossRef]

66. Kliukas, R.; Lukoševičienė, O.; Jaras, A.; Jonaitis, B. The Mechanical Properties of Centrifuged Concrete in Reinforced Concrete Structures. *Appl. Sci.* **2020**, *10*, 3570. [CrossRef]

67. Feng, B.; Zhu, Y.-H.; Xie, F.; Chen, J.; Liu, C.-B. Experimental Investigation and Design of Hollow Section, Centrifugal Concrete-Filled GFRP Tube Columns. *Buildings* **2021**, *11*, 598. [CrossRef]

68. Mailyan, L.R.; Stel'makh, S.A.; Shcherban, E.M. Differential characteristics of concrete in centrifugally spun and vibrospun building structures. *Mag. Civ. Eng.* **2021**, *108*, 10812. [CrossRef]

69. Beskopylny, A.N.; Stel'makh, S.A.; Shcherban', E.M.; Mailyan, L.R.; Meskhi, B.; Beskopylny, N.; El'shaeva, D.; Kotenko, M. The Investigation of Compacting Cement Systems for Studying the Fundamental Process of Cement Gel Formation. *Gels* **2022**, *8*, 530. [CrossRef]

70. Mailyan, L.R.; Stel'makh, S.A.; Shcherban', E.M.; Khalyushev, A.K.; Smolyanichenko, A.S.; Sysoev, A.K.; Parinov, I.A.; Cherpakov, A.V. Investigation of Integral and Differential Characteristics of Variatropic Structure Heavy Concretes by Ultrasonic Methods. *Appl. Sci.* **2021**, *11*, 3591. [CrossRef]

71. Shcherban', E.M.; Stel'makh, S.A.; Beskopylny, A.; Mailyan, L.R.; Meskhi, B. Influence of Mechanochemical Activation of Concrete Components on the Properties of Vibro-Centrifugated Heavy Concrete. *Appl. Sci.* **2021**, *11*, 10647. [CrossRef]

72. Zhong, Y.; Zhao, O. Behaviour of eccentrically loaded circular recycled aggregate concrete-filled stainless steel tube stub columns. *J. Constr. Steel Res.* **2022**, *198*, 107568. [CrossRef]

73. Jin, H.; Wei, Y.; Zhang, Y.; Huang, Z.; Liu, L. Compressive performance of underwater concrete columns strengthened by nondispersive mortar and stainless steel tubes. *Case Stud. Constr. Mater.* **2023**, *19*, e02220. [CrossRef]

74. Zhang, S.; Miao, K.; Wei, Y.; Xu, X.; Bin Luo, B.; Shi, W. Experimental and Theoretical Study of Concrete-Filled Steel Tube Columns Strengthened by FRP/Steel Strips Under Axial Compression. *Int. J. Concr. Struct. Mater.* **2023**, *17*, 1. [CrossRef]

75. More, F.M.D.S.; Subramanian, S.S. Experimental Investigation on the Axial Compressive Behaviour of Cold-Formed Steel-Concrete Composite Columns Infilled with Various Types of Fibre-Reinforced Concrete. *Buildings* **2023**, *13*, 151. [CrossRef]

76. Li, Q.; Liu, Z.; Zhou, X.; Wang, Z. Experimental Study and Finite Element Calculation of the Behavior of Special T-Shaped Composite Columns with Concrete-Filled Square Steel Tubulars under Eccentric Loads. *Buildings* **2022**, *12*, 1756. [CrossRef]